Accurate Boundary Localization using Dynamic Programming on Snakes

Akshaya Kumar Mishra, Paul Fieguth, D.A. Clausi
VIP research Group, Systems Design Engineering, University of Waterloo
Waterloo, ON, Canada
{akmishra, pfieguth, dclausi}@engmail.uwaterloo.ca

Abstract

The extraction of contours using deformable models, such as snakes, is a problem of great interest in computer vision, particular in areas of medical imaging and tracking. Snakes have been widely studied, and many methods are available. In most cases, the snake converges towards the optimal contour by minimizing a sum of internal (prior) and external (image measurement) energy terms. This approach is elegant, but frequently mis-converges in the presence of noise or complex contours.

To address these limitations, a novel discrete snake is proposed which treats the two energy terms separately. Essentially, the proposed method is a deterministic iterative statistical data fusion approach, in which the visual boundaries of the object are extracted, ignoring any prior, employing a Hidden Markov Model(HMM) and Viterbi search, and then applying importance sampling to the boundary points, on which the shape prior is asserted.

The proposed implementation is straightforward and achieves dramatic speed and accuracy improvement. Compared to four other published methods and across six different images (two original, four published), the proposed method is demonstrated to be, on average, 7 times faster with a 45 percent reduction in the mean square error. Only the proposed method was able to successfully segment the desired object in each test image.

Index Terms: ***Snake, Curvature guided importance sampling, HMM, Viterbi Algorithm, Statistical data fusion***

1. Introduction

Locating the exact boundaries of objects has many applications in object tracking [2], content based image and video retrieval systems [10, 9], robotics and biomedical engineering [7]. Energy minimizing splines, such as deformable snakes [11] or active contours, are the key approaches in the computer vision literature for such boundary extraction problems.

The principal idea in active contour modeling is to minimize the sum of internal (prior) and external (image-based) energies to obtain an optimum boundary. The internal energy typically asserts a first- or second-order smoothness constraint on the boundary, whereas the external energy applies a "force" on the boundary, creating an attractive force towards areas of high gradient. Since the original development of snake methods [11], many modifications have been attempted to overcome various shortcomings, primarily concentrated on altering the external energy, such as pressure based balloon force [5], distance transformed image gradient [6, 16], and gradient vector flow [18].

Amini [1] introduced the dynamic programming method for finding global minima of active contours taking advantage of the discrete nature of the problem. But, in dynamic programming approach it is difficult to incorporate complex shape priors. Further, Mortensen et.al [15] introduced intelligent scissor an user interactive dynamic programming based graph search method to locate exact boundary. This approach has limited use in automatic segmentations.

Traditional snakes have two problems. First, if the initial position is too far from the object boundary then the snake requires many iterations (and thus a long time) to converge, a particular concern in tracking or real-time problems. Second, standard snake algorithms do not guarantee convergence and tend to be very sensitive to noise and false weak edges. Both of these difficulties have seen considerable research attention, such as Gradient Vector Flow snake (GVFS) and the distance-transform based snake (DTS) of Cohen [6], designed to extend gradients throughout the image to lessen sensitivity to initialization, although the computational requirements are considerable. Similarly a balloon based pressure force [5] has been proposed which attracts active contours towards strong gradients, seeking to avoid noise and false gradients. However in both cases there remain a number of parameters for the user to tune, parameters which vary from image to image.

In this article a novel deformable model for the accurate localization of object boundaries is introduced. The method shares the same snake origins with conventional deformable

978-0-7695-3153-3/08 $25.00 © 2008 IEEE
DOI 10.1109/CRV.2008.13

models, however instead of minimizing the total energy of a snake like most existing methods, our method performs coordinate descent, alternately maximizing the external energy within a specified region, then applying the prior constraints to force the boundary to satisfy required smoothness. The adaptivity of the method to sharp corners is satisfied by importance sampling [13] the snake boundary points on the basis of curvature. Although our approach is parametric, users do not need to tune parameters for each image as the parameters are derived implicitly from image curvature and gradient. This proposed technique dramatically reduces computation time and dramatically improves the quality of the boundary solution compared to published snake methods irrespective of boundary geometry, image intensity and image noise.

The rest of paper is organized as follows. Section 2 briefly addresses conventional snakes. Section 3 explains the proposed method, results of which and comparisons to other methods are given in Section 4.

2 Snake Background

A deformable model or snake is a spline

$$\mathbf{v}(s) = [x(s), y(s)], s \in [0, L] \tag{1}$$

where s is the arclength along the snake and L is the total length of snake. The "Energy" of a given snake is given by

$$E_{total} = \int_0^L [E_{\text{int}}(\mathbf{v}) + \gamma E_{ext}(\mathbf{v})] ds \tag{2}$$

where we see two terms, an internal energy function

$$\mathrm{E}_{\text{int}}(\mathbf{v}) = \underbrace{\alpha \left| \frac{\partial \mathbf{v}}{\mathrm{ds}} \right|^2}_{elasticity} + \underbrace{\beta \left| \frac{\partial^2 \mathbf{v}}{\mathrm{ds}^2} \right|^2}_{rigidity} \tag{3}$$

which behaves like a prior model, a smoothness constraint on the snake, and a second energy term E_{ext}, which is the external image force, generally assigned as the negative gradient of image intensity ($-\nabla I$). The various parameters (α, β and γ) are weights, penalizing the slope or elasticity, curvature or rigidity, and external forces respectively. By definition, the optimum boundary is the one which minimizes E_{total}, whose closed form solution is not trivial (essentially impossible because of the clutter and complexity of the image term E_{ext}. Therefore, in the absence of closed-form solutions, iterative dynamic curve evolution methods are adopted to minimize E_{total} numerically.

A key problem, not currently addressed in the literature, is that parameters α, β and γ should really be functions of position, since the degree of curve smoothness, and the strength of the observed image gradient, can both be strong functions of location, nevertheless all existing methods considered these parameters to be constant. In our proposed method these parameters are chosen adaptively.

3 Proposed Method

This proposed method is briefly described by these three iterative steps. Details on each component follow.

1. The problem is modeled as a Hidden Markov Model (HMM) and a Viterbi search is used to find the optimal solution by dynamic programming. In the absence of image noise and shape prior, the Viterbi search will identify all of the strongest local boundaries. Details are developed in Section 3.1.

2. If spline points are uniformly spaced on the curve, there is an excess of points in areas of gentle curvature and too few points in areas of high curvature and complex structure. Thus, the curvature of the boundary, obtained from step one, is computed and importance sampling with specific rejection criteria is used to generate samples. Details are developed in Section 3.2.

3. The prior constraints need to be accounted and a trade-off between the strength and significance of the image gradients versus the smoothness desired by the prior must be established. Measurements at each sample location are acquired and assigned a weight based on the strength of the local gradient. The fused curve is estimated statistically. Details are found in Section 3.3.

3.1 Viterbi algorithm

The probability at each node in a trellis and an associated transition probability matrix define a hidden Markov model (HMM). Under the first order Markovian assumption, the Viterbi algorithm [17, 20] finds a sequence of nodes which maximizes the overall hypothesis. Terminology that defines the HMM in the context of a deformable snake model is provided next.

- A discrete snake is defined as a collection of $q-1$ discrete straight segments with q discrete locations (the head and tail of the snake do not have to be connected). An example of an initial snake is shown as a circle in Fig 1(a) and mathematically expressed as:

$$\mathbf{v}(s_b) = [x(s_b), y(s_b)], s_b \in [0, L], b \in [0, q-1] \tag{4}$$

- Assume a normal that crosses at each of the q discrete locations and that each normal has p nodes distributed

along its length. Each node represents a potential solution along that normal and, as a result, across all normals there are p^q potential solutions. Mathematically, $\mathbf{v_{ti}}$ is the i^{th} snake at iteration t:

$$\mathbf{v_{ti}}(s_b) = [x_{ti}(s_b), y_{ti}(s_b)], t \in [0, T-1], i \in [0, p^q] \tag{5}$$

- The trellis stores the state of the HMM. Let u_{ab} define the trellis which contains the positions of all potential snakes:

$$u_{ab} = \mathbf{v_{ti}}(s_b), a \in [-p/2, p/2] \tag{6}$$

The initial positions of a snake are $\mathbf{v_{00}}(s_b)$ represented as a circle in Fig 1(a). Here, small circles represent the trellis nodes. The external energy is calculated as the first derivative of a Gaussian kernel with $\sigma = 3pixels$. Mathematically, $E_{ext} = G_c^{'} * I$, where $E_{ext}, G_c^{'}, *$ and I are external force or the observations, Gaussian kernel of length c, convolution symbol and intensity of image respectively. The confusion matrix (B_{ab}) and state transition matrix A_{ab} are shown in (7) and (8) where $D(u_{kb-1}, u_{ab})$ is the Euclidian distance between u_{kb-1} and u_{ab}, $k \in [-p/2, p/2]$ is dummy variable used in Trellis.

$$B_{ab} = p(E_{ext}(u_{ab}) | E_{ext}(u_{k_{(-p/2:p/2)}b})) \tag{7}$$

$$A_{ab} = p(D(u_{ab}, u_{kb-1}) | D(u_{ab}, u_{k_{(-p/2:p/2)}(b-1)})) \tag{8}$$

Given observations E_{ext} of states u_{ab}, the goal is to find the best sequence of states $z_{\hat{a}b}$ which will maximize the probability function $\Re_{ab}$ along the path $z_{\hat{a}b}$ [8]. Mathematically, let $\Re_{ab}$ accumulate the likelihood at each node and $\Re_{a1} = B_{a1}$. With the assumption of a first order Markov model, $\Re_{ab}$, and knowledge of the previous likelihood path, O_{ab} can be computed using equation-(9) and (10).

$$\Re_{ab} = \max_{k_{(-p/2:p/2)}} (\Re_{k(b-1)} + A_{kb} B_{ab}) \tag{9}$$

$$O_{ab} = \arg\max_{k} (\Re_{k(b-1)} + A_{kb} B_{ab}) \tag{10}$$

The Viterbi algorithm computes the partial probability of each node in the trellis u_{ab}. By solving the forward problem [20], the sequence of the most likely occurring path $z_{\hat{a}b}$ is determined. Due to noise and first order Markov assumption the optimal snake obtained using the Viterbi method is typically not the desired snake. Therefore, a novel curvature based estimation technique is proposed which considers both curvature and prior shape model to pull the snake towards true positions.

3.2 Curvature guided importance sampling for curve evolution

In general, the prior model of objects are defined by constraints on its overall shape. Active contours traditionally consider thin plate and membrane constraints to constitute the prior model of the object which is not an accurate hypothesis for high curvature object boundaries. Therefore, the proposed method generates snake points using importance sampling of the local curvature(K) along the snake which will ensure more samples in high curvature regions. Importance sampling on the absolute value of curvature of $z_{\hat{a}b}$ is performed as described in (11), (12) and (13).

$$\rho_b \propto \frac{(q_b - q_{b-1})}{(s_b - s_{b-1})} \propto K \tag{11}$$

$$\Delta s_{min} < \Delta s < \Delta s_{max} \tag{12}$$

$$\frac{L}{\Delta s_{\max}} \ll q \ll \frac{L}{\Delta s_{\min}} \tag{13}$$

Δs_{min} and Δs_{max} represent the minimum and maximum length of a segment in a snake. Δs and ρ_b are the sampling interval and sample density. To estimate the true shape, the method measures at each location generated by importance sampling of $z_{\hat{a}b}$. The sample locations are assigned to M, as defined in the next subsection, which will be treated as measurements for further use.

3.3 Statistical estimation

There are two reasons motivating an estimation step. First, while calculating M, shape priors were not considered, however prior models of shapes play a vital role with high measurement uncertainty. Second, to directly incorporate complicated shape model directly into the Viterbi approach is difficult, even for second order constraint complexity. The new approach computes the object boundary from the observed image ignoring the prior model and then fuses the measured boundary with the prior model statistically. Let M be the measurement vector at sampled snake position and Z be the true boundary that needs to be estimated. M can be expressed as:

$$M = CZ + W \tag{14}$$

and an estimate of Z [4] is defined as:

$$\hat{Z} = (C^t R^{-1} C + P^{-1})^{-1} C^t R^{-1} M \tag{15}$$

where C is a rectangular matrix, W is the uncertainty in measurements, $W \sim N(0, R)$, P is the shape matrix which describes the object's prior model. The most difficult task is how to choose P and R. The first estimate for P includes elastic and membrane constraints:

$$P = \lambda(\pounds \pounds^t)^{-1} \tag{16}$$

where $\pounds$ is a penta-diagonal banded matrix which contains overall shape constraints:

$$\pounds = [\alpha(\mathbf{L_x} + \mathbf{L_y}) + \beta(\mathbf{L_{xx}} + \mathbf{L_{yy}})] \tag{17}$$

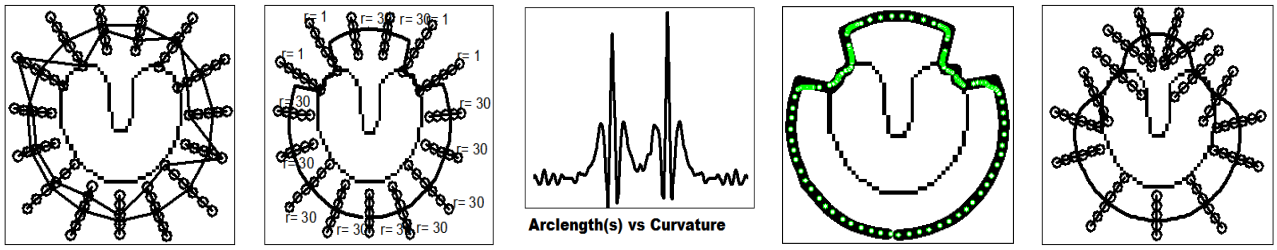

(a) (b) (c) (d) (e)

Figure 1. Illustration of one iteration of proposed method on a U-shaped object. (a) A circle (thick line) shows the initial positions of the snake, the jagged line shows a potential snake solution, and the small circles shows the nodes of Viterbi trellis. (b) The thick line shows the optimal snake after a Viterbi search. (c) Curvature of the curve obtained using Viterbi search (X-axis Arc length, Y-axis Curvature(K)). (d) small green circles are the particles generated using importance sampling on curvature of optimal Viterbi snake. (e) The thick line shows the estimated snake as the initial snake to start the next iteration.

Algorithm 1 Pseudo code of proposed method

1: $t = 0$, $e = \infty$, $\epsilon = 1^{(-10)}$
2: Initialize object boundary manually as $\mathbf{v_{00}}(s)$
3: **while** $e \geq \epsilon$ **do**
4: Generate discrete search space u_{ab} normal to $\mathbf{v_{t0}}(s)$
5: Find the best curve $z_{\hat{a}b}$ using Viterbi search
6: Compute curvature of $z_{\hat{a}b}$ and perform importance sampling on it to generate more sample near high curvature region. Consider each sample as measurements(M)
7: Calculate $\hat{z(t)}$
8: $e = ||\hat{z}(t) - \hat{z}(t-1)||$
9: $\mathbf{v_{(t+1)0}}(s) = \hat{z}(t)$
10: $t = t + 1$
11: **end while**

$\mathbf{L_x}, \mathbf{L_{xx}}, \mathbf{L_y}$, and $\mathbf{L_{yy}}$ are shape elastic and membrane constraints along the x and y direction. $\mathbf{L_x}, \mathbf{L_{xx}}, \mathbf{L_y}$, and $\mathbf{L_{yy}}$ are banded matrices whose values at center rows are $[1, -1], [1, -2, 1], [1, -1]^t$ and $[1, -2, 1]^t$ respectively. λ is weight factor for shape constraints. Further, R is a diagonal matrix whose diagonal elements $r_{11}, r_{22}...r_{bb}...r_{qq}$ are derived from the probability distribution of external force.

$$r_{bb} \propto \frac{1}{E_{ext}} \tag{18}$$

In principle r_{bb} have lower values in regions where the external forces are high. Pseudo code for complete approach is provided in Algorithm (1)

4 Testing

4.1 Test images and initialization

To authenticate the capability of the proposed method, testing has been conducted on both original and published images. Two synthetic binary images are tested, one with a V shaped object and the other with a heart shaped object. The four standard images are brainweb [12], disc on a complex background [16], starfish [3], thin u-shape [18]. The labels A, B, C, D, E and F are assigned to V-shape, heart shape, ball in complex background, brain, starfish and thin u-shape images, respectively, as illustrated in Fig. 2. Experiments are performed on 2.61 GHZ, 2GB DD RAM, AMD Athlon 64X2 dual core machine .

For comparison purposes, published MATLAB code for the Gradient Vector Flow (GFV) snake, Traditional snake, Balloon Force (BF) snake and Distance Transformed Force (DTF) snake were downloaded [19]. The downloaded original codes took a long time to run and we modified them to perform vector optimization within MATLAB to fairly compare completion times against the proposed method's implementation. The initial location of the snake is always specified using a circle. The initial length of each segment is Δs. For all test images values of Δs_{min} and Δs_{max} are set to be 0.5 pixels and 3 pixels. The minimum and maximum values of r_{bb} are set to 1 and 30. Parameters for the other four methods were set according to [18] and fixed for all test sets.

4.2 Results

Results are shown in Fig. 2 and Table 1. Fig. 2 illustrates separate images for the initial contour, the solution for the proposed method, and the solution for the four other methods. Table 1 shows the quantitative values of Mean Square Error (MSE) and Execution Time (ET) of all five methods.

In the proposed method, parameters of the discrete snake are guided by curvature and external force. As a result, the proposed method works effectively for all six images without adjusting any parameters. In contrast, the four comparative methods are sensitive to fixed parameters and no other method can effectively identify the necessary boundary for

Table 1. Comparison table showing Mean Square Error(MSE) and Execution Time (ET) in second of Proposed Method against four other methods for different images. Text in bold letter indicates best performance among their peers for a particular image

	Proposed Snake		Traditional Snake		DTF Snake		BF Snake		GVF Snake	
	MSE	ET	MSE	ET	MSE	ET	MSE	ET	MSE	ET
(A)	**0.89**	**14**	1.4	91	110	42	1.4	93	1.1	112
(B)	**1.1**	**29**	2.9	91	2.6	36	1.2	93	2.5	104
(C)	**1.5**	**4.5**	1.55	36	DNC	38	DNC	70	1.53	52
(D)	**1.8**	**3.5**	1.83	47	2.1	46	1.9	42	1.85	73
(E)	**2.1**	**26**	42	145	DNC	40	DNC	119	351	171
(F)	**2.7**	**31**	12	91	16	48	9.5	94	6	114

all test images. In particular, only the proposed method found the appropriate boundary for the starfish (E) image. The starfish shape (E) has a complex boundary and also has an intensity that is highly non-uniform. The disc (C) poses challenges with a variety of edge strengths throughout the image and two of the methods (DTF snake and BF snake) did not converge for this image, however, the proposed method successfully segments the object. For some cases, the algorithm did not converge (DNC), which means that the snake shrunk to a single point or expanded outside of the image plane.

Table 1 shows that the proposed method gives the best performance for both speed and MSE for all images across all snake algorithms. On average, across all images and compared to all snake methods, the proposed method is found to be 7 times faster with a 45 percent reduction in MSE.

4.3 Algorithm sensitivity

- Sensitivity to initial position:

  Typically, for the proposed method to be effective, the initial snake is of reasonable size with a boundary covering its solution boundary. Fig. 3 shows three different initial snake contours and their successful convergence using the proposed method. In contrast, the balloon force (BF) snake requires that the initial snake be placed fully within the solution boundary [18]. Also, the Traditional snake requires an initial snake close to its solution to encourage speed of convergence and accuracy [18]. Further, slower convergence speed is a consistent concern for the GVF snake method.

- Sensitivity to parameter change:

  Performance of existing contour extraction techniques are dependent upon appropriate values of parameters such as α, β and γ. However, the proposed method adaptively chooses parameters as given below where ρ_b (11) and r_{bb} are functions of spatial locations.

$$[\alpha, \beta, \lambda] \propto \rho_b \tag{19}$$

and

$$[\alpha, \beta, \lambda] \propto \frac{1}{r_{bb}} \tag{20}$$

therefore, α, β and λ also function of spatial locations. The proposed method does not have γ term, because external and internal forces are decoupled. While computing the visual boundary of an object γ is embedded implicitly within the trellis of HMM. However $\frac{\alpha}{\beta}$ is significant for rate of convergence which is beyond the scope of the article. Therefore, in our experiment α,β, and λ are set to be 0.28, 0.04 and 1 to accomplish reasonable advantage on speed.

A thorough rigorous experiment has been conducted to understand the effect of parameter estimation on the final solution for each of the five methods. That the final solution of the proposed method does not vary significantly for a wide range of parameters within the domain of our test case has been observed. However, for other methods, proper values of parameters are important for the snake to converge to the true solution. As a result, the proposed method is less sensitive to parameter changes, while other methods are more sensitive to these parameters.

- Sensitivity to noise:

  Fig. 4 shows the effect of varying noise on mean square error (MSE) as a function of the number of iterations given the binary diamond shape in Fig. 5. For lower values of noise variance (higher values of PSNR), the proposed method takes less time to converge. Fig. 5 compares the proposed method to the other four methods for a PSNR of 6 given a noisy image with a diamond shape. Clearly, the proposed method is robust to noise relative to its peers since the proposed method is the only method to successfully identify the diamond.

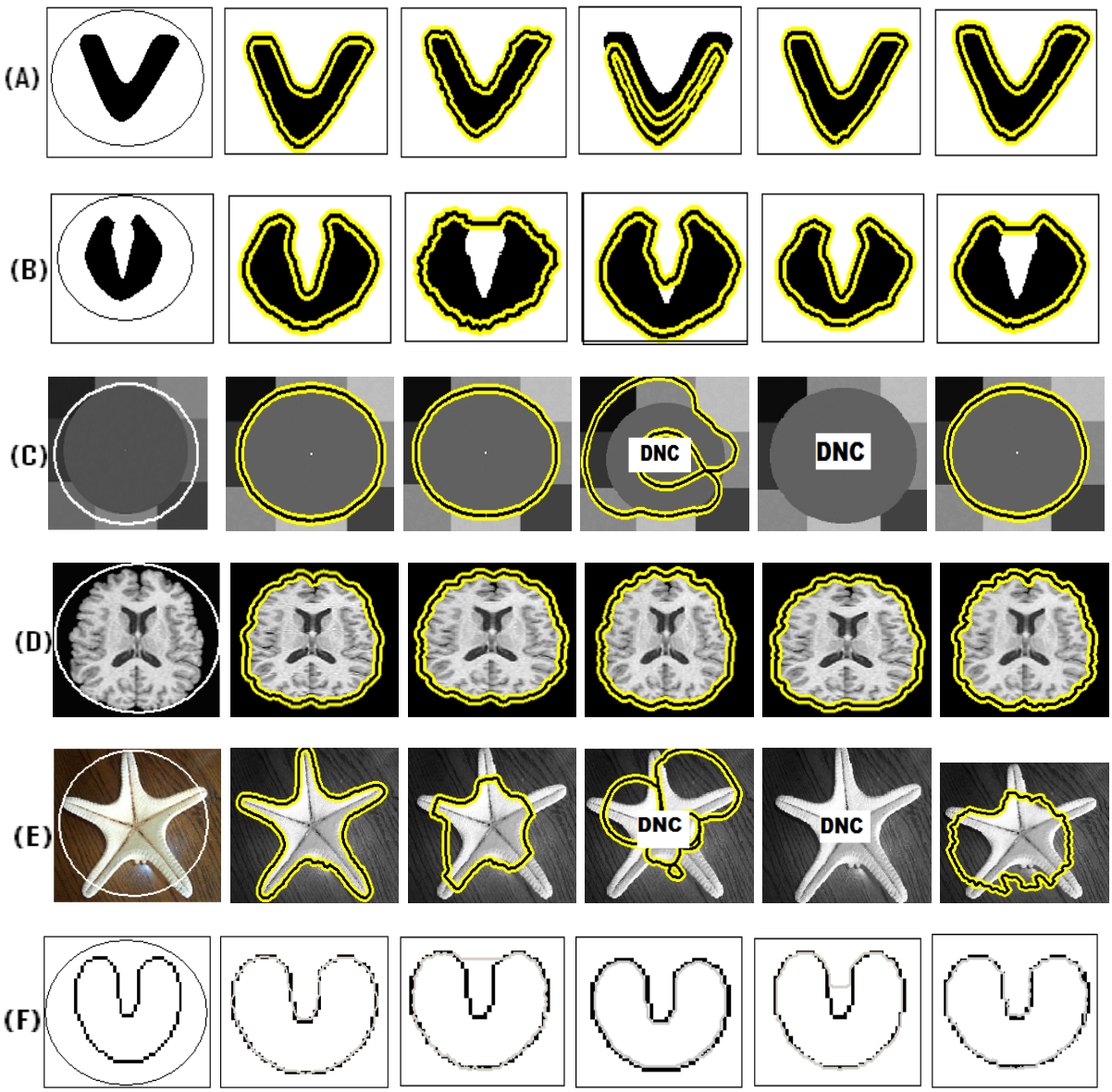

Figure 2. Column 1 shows the initial circular snake; column 2 the snake generated using the proposed method; column 3 to 6 shows results using four other snake techniques [11, 5, 6, 18]. Black lines bounded by yellow lines are final contours. First two rows (A and B) show two synthesized images. Last four rows (C, D, E, and F) show images obtained from [16, 18, 12, 3]. The proposed method is the only one that can properly identify the object boundary in each case. No other method works for more than four images. Some test cases did not converge

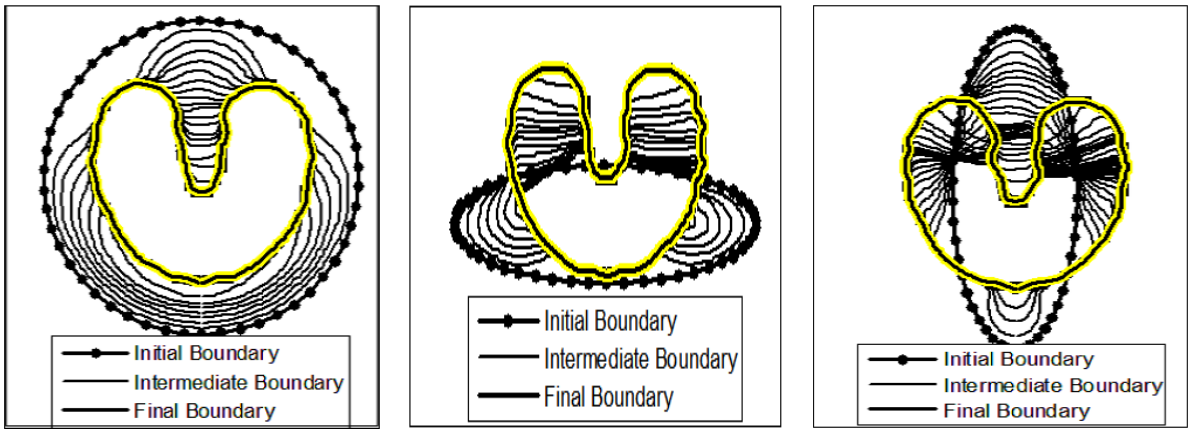

(a) (b) (c)

Figure 3. Behaviour of convergence pattern of proposed snake on initial positions for a u-shaped object.

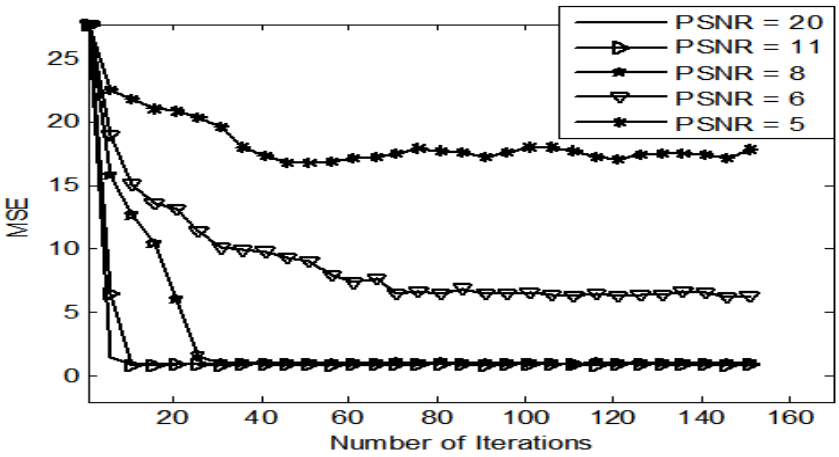

Figure 4. Effect of noise PSNR on convergence time and MSE for proposed snakes to converge using image in Fig. 5. Range of intensity of image is between 0 and 1.

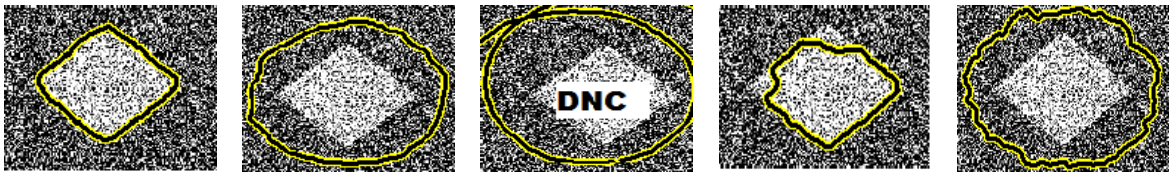

Proposed Snake **Traditional Snake [11]** **DTF Snake [6]** **BF Snake [5]** **GVF Snake [18]**

Figure 5. Performance of each method in presence of noise with $\sigma = 0.65$, $\mu = 0.1$, and PSNR = 6. Only the proposed method works effectively in the noisy image.

5 Conclusions and Future Efforts

A novel discrete snake for accurate boundary extraction regardless of noise and geometry of the object boundary is designed and implemented. This discrete snake adjusts its parameters iteratively as a function of the current snake solution. Each iteration of the discrete snake is carried out in three steps: Viterbi search, importance resampling, and statistical estimation. Validation of the proposed method is demonstrated experimentally using two original synthetic images and other four published images. The method is demonstrated to be robust to initial parameter setting regardless of the nature of the image. Convergence of proposed method is guaranteed empirically and robustness to noise is shown experimentally.

In the future, parametric testing will be conducted to better understand the contribution of each parameter to the final solution. A design that can enable identification of boundaries for images with multiple objects is also under consideration.

6 Acknowledgements

This work has been supported by GEOIDE (Geomatics for Informed Decisions) an NSERC Network of Centres of Excellence. We are grateful to Nezam Kachouie and Alexander Wong for their assistance.

References

[1] A. A. Amini. *Using dynamic programming for solving variational problems in vision: applications involving deformable models for contours and surfaces.* PhD thesis, Ann Arbor, MI, USA, 1990.

[2] A. A. Amini, R. W. Curwen, and J. C. Gore. Snakes and splines for tracking non-rigid heart motion. In *Computer Vision - ECCV'96, 4th European Conference on Computer Vision*, pages 251–261, Cambridge, UK, 1996.

[3] K. Bay. Starfish- they are huge, Sept. 2007. http://kahunabay.wordpress.com/2007/09/07/starfish-they-are-huge/.

[4] M. Bertero, C. De Mol, and E. R. Pike. Linear inverse problems with discrete data. II. Stability and regularisation. *Inverse Problems*, 4(3):573–594, 1988.

[5] L. D. Cohen. On active contour models and balloons. *CVGIP:Image Understanding*, 53(2):211–218, March 1991.

[6] L. D. Cohen and I. Cohen. Finite-element methods for active contour models and balloons for 2-d and 3-d images. *IEEE Trans. on Pattern Anal. Mach. Intell.*, 15(11):1131–1147, 1993.

[7] C. A. Davatzikos and J. L. Prince. An active contour model for mapping the cortex. *IEEE Trans. on Medical Imaging*, 14(1):65–80, March 1995.

[8] J. Hagenauer and P. Hoeher. A Viterbi algorithm with soft-decision outputs and its applications. volume 3, pages 1680–1686, 1989.

[9] K. Hirata, E. Kasutani, and Y. Hara. On image segmentation for object-based image retrieval. In *International Conference on Pattern Recognition, Quebec city, Quebec, Canada*, pages III: 1031–1034, 2002.

[10] J. Ho and W. Hwang. Segmenting microarray image spots using an active contour approach.

[11] M. Kass, A. Witkin, and D. Terzopoulos. Snakes: Active contour models. *International Journal of Computer Vision*, 1(4):321–331, 1988.

[12] R. Kwan, A. Evans, and G. Pike. MRI simulation-based evaluation of image-processing and classification methods. 18(11):1085–1097, November 1999.

[13] E. A. Lehmann and R. C. Williamson. Particle filter design using importance sampling for acoustic source localisation and tracking in reverberant environments. *EURASIP J. Appl. Signal Process.*, 2006(1):168–168, 2005.

[14] R. Malladi, J. A. Sethian, and B. C. Vemuri. Shape modeling with front propagation: A level set approach. *IEEE Trans. on Pattern Anal. Mach. Intell.*, 17(2):158–175, 1995.

[15] E. N. Mortensen and W. A. Barrett. Intelligent scissors for image composition. In *SIGGRAPH '95: Proceedings of the 22nd annual conference on Computer graphics and interactive techniques*, pages 191–198, New York, NY, USA, 1995. ACM.

[16] F. Y. Shih and K. Zhang. Locating object contours in complex background using improved snakes. *Computer. Vision. Image Underst.*, 105(2):93–98, January 2007.

[17] A. J. Viterbi. Error bounds for convolutional codes and an asymptotically optimum decoding algorithm. *IEEE Trans. on Information Theory*, IT-13:260–269, 1967.

[18] C. Xu and J. Prince. Snakes, shapes, and gradient vector flow. *IEEE Trans. on Image Processing.*, 7(3):359–369, March 1998.

[19] C. Xu and J. L. Prince. Johns hopkins university, image analysis and communications lab, gvf software, Sept. 1999. http://iacl.ece.jhu.edu/projects/gvf/.

[20] G. Zhou and J. Su. Named entity recognition using an hmm-based chunk tagger. In *ACL '02: Proceedings of the 40th Annual Meeting on Association for Computational Linguistics*, pages 473–480, 2001.